Int. J. Non-Linear Mechanics, Vol. 24, No. 1, pp. 41–56, 1989
Printed in Great Britain.

0020-7462/89 $3.00 + 0.00
Pergamon Press plc

THE TRANSITION TO CHAOS IN A SIMPLE MECHANICAL SYSTEM

STEVEN W. SHAW*

Department of Mechanical Engineering, Michigan State University, East Lansing, MI 48824, U.S.A.

and

RICHARD H. RAND†

Department of Theoretical and Applied Mechanics, Cornell University, Ithaca, NY 14853, U.S.A.

(*Received* 20 *May* 1988; *accepted for publication* 15 *July* 1988)

Abstract—A simple mechanical device and its response to periodic excitation is considered. The system consists of an inverted pendulum with rigid barriers which limit the amplitude variation from the unstable upright position. The static stable rest positions correspond to the pendulum leaning against one of the barriers. When subjected to periodic excitation the system response can be quite complicated and may include one or several stable subharmonics and or chaotic motions. The analysis presented here is based on a piecewise linear model which allows explicit analytic expressions to be determined for many bifurcation conditions including: the appearance of certain types of subharmonics by saddle-node bifurcations, the secondary bifurcations of these subharmonics, and a global bifurcation which results in the creation of horseshoes.

1. INTRODUCTION

Even for simple driven non-linear oscillators the determination of periodic responses, their stability, and bifurcations from them is generally a formidable, if not impossible, task. Digital simulations must be employed unless one is considering a system which is a perturbation of an integrable one [1, 2]. Here we present an example of a system which is piecewise linear and for which explicit solutions are known locally and are matched together to obtain a "complete" solution. This type of formulation allows an implicit form of a Poincaré map to be obtained and from this map we obtain explicit results regarding existence and stability of certain periodic motions. The Poincaré map used here is not the usual one which samples the phase space once per period of the forcing. Instead a map is used which can capture some types of periodic motions of very long period in a single iterate. Using this map we can also compute the condition for the onset of chaotic motions using a Melnikov analysis. We relate these two kinds of results in the following way: firstly we obtain conditions for the existence of two distinct types of periodic motions. For each type we obtain the linearization of the Poincaré map at the associated fixed point and use this to examine the stability of the corresponding periodic motion. Accompanying a change in stability is a bifurcation which gives rise to a change in a number of solutions and in their periods. By setting the eigenvalues of the linearized map equal to ± 1 (the condition for stability change), we obtain conditions for such a bifurcation to occur. In this way we obtain a formula for the appearance of subharmonics of order n through saddle-node bifurcations, and the loss of stability of such motions through period doubling (Type I) or pitchfork bifurcations (Type II). Then we take the limit of these bifurcation formulas as $n \to \infty$, and find that each gives the same limiting expression, a condition for the existence of periodic motions with arbitrarily long period. This latter result is identical to that obtained by Melnikov analysis, i.e. by requiring the stable and unstable manifolds of a key periodic motion to intersect.

Because of the piecewise linear nature of the problem, all our results are obtainable in *exact* analytic form. Similar results for nearly integrable systems have been treated by

Contributed by P. Hagedorn.
Partially supported by:
*NSF grant MEA-8421248 and by DARPA.
†NSF, AFOSR and ARO through MSI.

Greenspan and Holmes [2] and Chow *et al.* [1]. In contrast, the results presented here do not depend on small parameter assumptions or on topological arguments.

The paper is outlined as follows: the physical system and model are described in Section 2. The Poincaré map is defined in Section 3, the existence of two types of periodic responses is considered in Section 4 and a stability and bifurcation analysis is given in Section 5. Section 6 describes the Melnikov analysis, the results from simulations are presented in Section 7, and we close with a discussion in Section 8.

2. DESCRIPTION OF THE PROBLEM

The physical system under consideration is depicted in Fig. 1. It consists of a simple inverted pendulum with rigid barriers on either side of the unstable equilibrium position. The static equilibria are the states in which the pendulum is resting against either wall. The system is forced with a horizontal sinusoidal motion as shown. For small excitation amplitudes one expects the motion to be a simple bouncing or leaning against one wall and for large excitation the pendulum will interact with both walls in some manner. The transition region contains rich dynamical behavior.

The non-dimensional equations of motion are

$$\ddot{x} + 2\alpha\dot{x} - x = \beta \cos \omega t \qquad |x| < 1 \tag{1a}$$

$$\dot{x} \to -r\dot{x} \qquad |x| = 1 \tag{1b}$$

where α is a linear damping coefficient, β is the forcing amplitude and $r \leqslant 1$ is a reflection coefficient representing energy lost during impact. Length and time have been rescaled such that the barriers are a unit distance from the vertical equilibrium position and the time constant of the pendulum is unity. We have assumed that the barriers are close enough so that linearization is valid during free flight (this is the only small parameter assumption needed here). Encounters with the barrier have been modeled by using the simple impact rule (1b) which assumes instantaneous impact with some energy loss.

The unperturbed system is taken to be the unforced, undamped system

$$\ddot{x} - x = 0, \qquad |x| < 1$$

$$x \to -x \qquad |x| = 1.$$

The phase plane for this case is shown in Fig. 2. Note that the unperturbed system is topologically equivalent to that for Duffing's equation which has been studied extensively by Holmes and his co-workers (see [2, 4, 5] for example) and by Chow *et al.* [1] for small β and α. Salam [6] presents results which extend the analysis to include large dissipation, but still require small forcing. Here, as in Chow and Shaw [7] for the Josephson junction, we allow large dissipation and large excitation amplitude.

In Fig. 2 it is seen that there exist orbits with periods ranging from zero at the infinite velocity limit to infinity along the homoclinic orbits. The orbits inside the homoclinic trajectories also have periods which vary from infinity at the homoclinic orbits to zero at each rest point. When the excitation and damping are added these periodic orbits provide

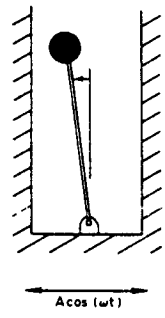

Fig. 1. The physical system.

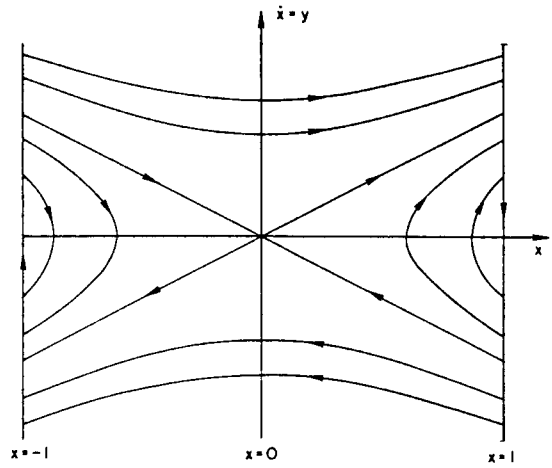

Fig. 2. The unperturbed phase portrait.

the "base" motions from which subharmonic motions arise. Perturbations of the homoclinic orbits result in the appearance of chaotic motions [1, 2].

3. THE POINCARÉ MAP

Rewriting equation (1) in first order form, the (x, y, φ) phase flow is governed by

$$\left.\begin{aligned}\dot{x} &= y\\ \dot{y} &= x - 2\alpha y + \beta\cos\omega\varphi\\ \dot{\varphi} &= 1\end{aligned}\right\} \quad |x| < 1 \tag{2a}$$

$$(x, y, \varphi) \to (x, -ry, \varphi) \qquad |x| = 1 \tag{2b}$$

where $\varphi = t(\mathrm{mod}\, T)$, $T = 2\pi/\omega$.

We shall denote the solution to (2) corresponding to the initial conditions $x = x_0$, $y = y_0$, $\varphi = \varphi_0$ by

$$x = x(t; x_0, y_0, \varphi_0), \quad y = y(t; x_0, y_0, \varphi_0).$$

The Poincaré section is taken to be:

$$\Sigma = \{(x, y, \varphi) \in I \times \mathbb{R} \times S \,|\, x = +1, y > 0\} = \mathbb{R}^+ \times S$$

where $I = [-1, 1]$ and S is the circle of period T, see Fig. 3. This is a natural choice and is prompted by the nature of the vector field given by (2). Elements in Σ are denoted by $(y, \varphi) \in \mathbb{R}^+ \times S$.

Consider a point $(y, \varphi) \in \Sigma$. It is immediately mapped to $(-ry, \varphi) \notin \Sigma$ under the impact rule (2b). Then, under the flow of equation (2a), it returns to Σ after a free flight of duration τ, corresponding to the next time that the associated motion intersects the cut $x = +1$ with $y > 0$:

$$\tau(y, \varphi) = \inf\{t > 0 \,|\, x(t; +1, -ry, \varphi) = +1, y(t; +1, -ry, \varphi) > 0\}.$$

The Poincaré map is thus given by

$$\mathbf{P}(y, \varphi) = (y(\tau(y, \varphi); +1, -ry, \varphi), \tau(y, \varphi) \,(\mathrm{mod}\, T)).$$

See [7–10] for analyses using similarly defined maps. Some remarks regarding $\mathbf{P}$:

(1) There is one periodic motion which is not captured by $\mathbf{P}$. It is given for $\beta < q$ by the following particular solution of (1):

$$\tilde{x} = \gamma\cos(\omega t + \psi)$$

$$\tilde{y} = \gamma\omega\sin(\omega t + \psi)$$

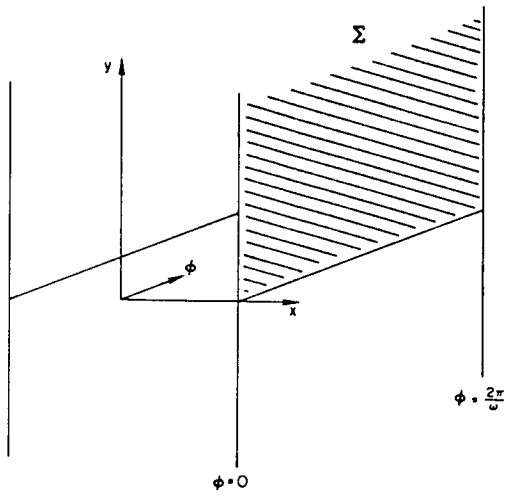

Fig. 3. The extended phase space (x, y, φ) and the Poincaré section Σ.

where $\gamma = \beta/q, q = [(1+\omega^2)^2 + (2\alpha\omega)^2]^{1/2}$, and $\tan\psi = \dfrac{2\alpha\omega}{1+\omega^2}$. This motion has a saddle type orbit and is the analytic continuation in β, about $\beta = 0$, of the origin in the unforced problem. For $\beta < q$ this is a non-impacting periodic motion of period T. Its stable and unstable manifolds play a central role in the birth of long period motions and horseshoes.

(2) The return time τ depends on the starting point $(y, \varphi) \in \Sigma$ and may be arbitrarily long if the trajectory is started close to the stable manifold of the saddle orbit. This is precisely how long period subharmonics are captured using **P**.

(3) Points in Σ correspond to the pendulum impacting on the barrier at $x = +1$. We denote by y the velocity just prior to impact, and by φ the forcing phase at impact. Then the velocity just subsequent to imapct is $-ry$.

(4) **P** is not a "nice" mapping since there are points in Σ which are mapped to $x = \pm 1$, $y = 0$. Such points correspond to degenerate impacts which barely kiss a wall, and these lead to discontinuities in the map, see [10, 11].

(5) **P** captures motions which go to $x = -1$ (possibly several times) and return to $x = +1$.

(6) However, **P** misses points which end up impacting only at $x = -1$. Nevertheless, due to the symmetry of the system, **P** will find such a motion's antisymmetric partner which impacts only at $+1$.

(7) **P** is known in implicit form only, since the process of obtaining $\tau(y, \varphi)$ requires finding the root(s) of one or more transcendental equation(s).

A simple analysis indicates that the system admits, for small β, a "semi-static" motion in which the pendulum mass simply rests against one of the barriers and moves with it. The condition for the existence of such a motion, determined by examining the dynamic contact force between the pendulum mass and a barrier, is given by $\beta \leqslant 1$. Thus for any parameters satisfying $\beta \leqslant 1$, one must consider the possibility of this motion. Its basin of attraction shrinks, no doubt, as $\beta = 1$ is approached from below. This motion will be denoted as the *rest solution* in the following.

4. PERIODIC MOTIONS

There exist many types of possible periodic motions involving impacts at $x = +1$ and -1. Here we consider only those which are captured in a single iterate of **P**. In Fig. 4 are shown, in the x–y phase plane, the two types of such motions. Type I periodic motions correspond to the pendulum bouncing repeatedly at the $x = +1$ (or -1) wall with free flight time of nT between each impact. Type II periodic motions are symmetric and bounce back and forth between both walls with times of flight of $nT/2$ between each impact. Conditions for the existence and stability for each type can be expressed in closed form.

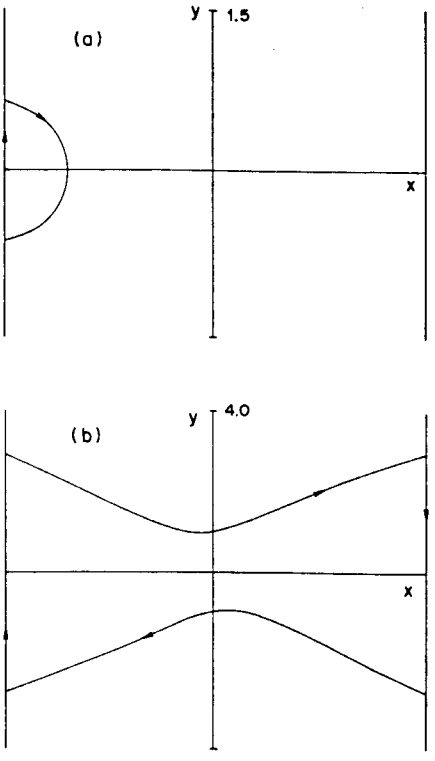

Fig. 4. Simple periodic motions with $r = 1.0$, $\alpha = 0.1$. (a) Type I motion, $\beta = 0.6$, $\omega = 4.0$, period T. (b) Type II motion, $\beta = 2.3$, $\omega = 1.95$, period T.

4.1. *Type I motions*

Conditions for the existence of a period nT subharmonic motion of Type I are given as follows in terms of a point $(y_n, \varphi_n) \in \Sigma$:

$$x(\varphi_n + nT; +1, -ry_n, \varphi_n) = +1 \tag{3a}$$

$$y(\varphi_n + nT; +1, -ry_n, \varphi_n) = y_n \tag{3b}$$

$$|x(\varphi_n + t; +1, -ry_n, \varphi_n)| < 1, \qquad 0 < t < nT. \tag{3c}$$

In words, equations (3) specify a motion which starts at $x = +1$, $y = y_n$ and $t = \varphi_n$, which immediately takes on the velocity $-ry_n$ by the impact rule (2b), and which returns to $x = +1$, $y = y_n$ after travelling for a time nT without touching the walls $x = \pm 1$.

Theorem 1. A point $(y_n, \varphi_n) \in \Sigma$ is a fixed point of **P** and corresponds to a Type I subharmonic of order n if the following are satisfied

$$[I_n^2 + \omega^2 G_n^2]\, y_n^2 - 2G_n H_n \omega^2 y_n + \omega^2 H_n^2 \left[1 - \frac{\beta^2}{q^2}\right] = 0 \tag{4a}$$

$$\sin(\omega\varphi_n + \psi) = -y_n I_n q/\beta\omega H_n \tag{4b}$$

$$\cos(\omega\varphi_n + \psi) = (H_n - y_n G_n) q/\beta H_n \tag{4c}$$

where

$$H_n = \cosh(nT\Omega) - \cosh(nT\alpha)$$

$$G_n = \frac{1+r}{2\Omega} \sinh(nT\Omega)$$

$$I_n = \frac{1-r}{2} H_n + \left[\frac{1+r}{2}\right]\left[\frac{\alpha}{\Omega} \sinh(nT\Omega) - \sinh(nT\alpha)\right]$$

$$\Omega = [1 + \alpha^2]^{1/2}.$$

Proof (outline): the solution of equation (1a) based at $(x, y, t) = (+1, -ry_n, \varphi_n)$ is given by

$$x(t;\ +1, -ry_n, \varphi_n) = e^{-\alpha(t-\varphi_n)}\left[A\cosh[\Omega(t-\varphi_n)] + B\sinh[\Omega(t-\varphi_n)]\right] + \frac{\beta}{q}\cos(\omega t + \psi) \tag{5}$$

where

$$A = 1 - \gamma\cos(\omega\varphi_n + \psi)$$

$$B = [-ry_n + \gamma\omega\sin(\omega\varphi_n + \psi) + \alpha A]/\Omega.$$

Using (5) and its time derivative, conditions (3a) and (3b) can be algebraically rearranged to obtain two equations which involve y_n, φ_n and the system parameters. These equations are linear in y_n, $\sin(\omega\varphi_n + \psi)$ and $\cos(\omega\varphi_n + \psi)$. Solving them for the sine and cosine gives equations (4b) and (4c). Then $\sin^2(\ ) + \cos^2(\ ) = 1$ results in condition (4a). See [7] for more details of a similar calculation.

From equation (4a) it is seen that there exist at most two real solutions for y_n. Only at saddle-node points does only one solution for y_n exist and the conditions for such are easily obtained. It should be reiterated that Type I orbits exist in pairs due to symmetry, one associated with $x = +1$ and the other with -1. Thus each root y_n of (4a) corresponds to a pair of Type I motions.

Corollary 2. Saddle-node bifurcations which result in the appearance of pairs of Type I subharmonics of order n occur at

$$\beta_n^I(\mathrm{SN}) = \frac{q|I_n|}{[I_n^2 + \omega^2 G_n^2]^{1/2}}. \tag{6}$$

For $\beta > \beta_n^I(\mathrm{SN})$ two pairs of such subharmonics exist. In Section 5 the stability of these will be considered.

Corollary 3. The limit $n \to \infty$ for $\beta_n^I(\mathrm{SN})$ gives

$$\beta_\infty = \frac{q|(1-r)\Omega + (1+r)\alpha|}{[((1-r)\Omega + (1+r)\alpha)^2 + (\omega(1+r))^2]^{1/2}} \tag{7}$$

and corresponds to the appearance of arbitrarily long periodic motions. In Section 6 this result is compared with a Melnikov analysis.

4.2. *Type II motions*

The following conditions must hold for the existence of a symmetric subharmonic motion of Type II:

$$x\left(\varphi_n + \frac{nT}{2};\ +1, -ry_n, \varphi_n\right) = -1 \tag{8a}$$

$$y\left(\varphi_n + \frac{nT}{2};\ +1, -ry_n, \varphi_n\right) = -y_n \tag{8b}$$

$$\left|x\left(\varphi_n + t;\ +1, -ry_n, \varphi_n\right)\right| < 1, \qquad 0 < t < \frac{nT}{2}. \tag{8c}$$

Theorem 4. A point $(y_n, \varphi_n) \in \Sigma$ is a fixed point of P and corresponds to a Type II subharmonic of order n if the following are satisfied

$$(K_n^2 + \omega^2 L_n^2)\, y_n^2 - 2L_n J_n \omega^2 y_n + \omega^2 J_n^2\left(1 - \frac{\beta^2}{q^2}\right) = 0 \tag{9a}$$

$$\sin(\omega\varphi_n + \psi) = -y_n K_n q/\beta\omega J_n \tag{9b}$$

$$\cos(\omega\varphi_n + \psi) = (J_n - y_n L_n)q/\beta J_n \tag{9c}$$

where

$$J_n = \cosh\left(\frac{nT\Omega}{2}\right) + \cosh\left(\frac{nT\alpha}{2}\right)$$

$$L_n = \frac{1+r}{2\Omega}\sinh\left(\frac{nT\Omega}{2}\right)$$

$$K_n = \frac{1-r}{2}J_n + \left(\frac{1+r}{2}\right)\left(\frac{\alpha}{\Omega}\sinh\left(\frac{nT\Omega}{2}\right) + \sinh\left(\frac{nT\alpha}{2}\right)\right)$$

The proof of Theorem 4 is similar to that of Theorem 1 and is not given.

Corollary 5. Saddle-node bifurcations which result in the appearance of pairs of Type II subharmonics of order n occur at

$$\beta_n^{II}(\mathrm{SN}) = \frac{q|K_n|}{(K_n^2 + \omega^2 L_n^2)^{1/2}}. \tag{10}$$

For $\beta > \beta_n^{II}(\mathrm{SN})$ one pair of such subharmonics exist. The stability of these motions is considered in Section 5.

The limit $n \to \infty$ gives condition (7) once again. This implies that saddle-node bifurcations for both types of orbits accumulate onto the same condition as n increases. This is discussed more fully in Section 6.

The stability of these periodic motions and secondary bifurcations from them are now considered.

5. STABILITY AND SECONDARY BIFURCATIONS OF PERIODIC MOTIONS

In this section the first derivative DP of the return map $\mathbf{P}$ is computed and its eigenvalues examined. This derivative is computed via implicit differentiations.

5.1. *Type I motions*

Let $(y_2, \varphi_2) = \mathbf{P}(y_0, \varphi_0)$ with $(y_1, \varphi_1) = (-ry_0, \varphi_0)$, and $\varphi_j = t_j (\mathrm{mod}\, T)$.

Then y_2 and φ_2 are defined as implicit functions of y_1 and φ_1 by the conditions

$$x(t_2; +1, y, \varphi_1) = +1 \tag{11a}$$

$$y(t_2; +1, y_1, \varphi_1) = y_2. \tag{11b}$$

Differentiation with respect to (y_1, φ_1), using expression (5) and its time derivative, gives the Jacobian

$$\begin{bmatrix} \dfrac{\partial t_2}{\partial \varphi_1} & \dfrac{\partial t_2}{\partial y_1} \\ \dfrac{\partial y_2}{\partial \varphi_1} & \dfrac{\partial y_2}{\partial y_1} \end{bmatrix} = \begin{bmatrix} \dfrac{\partial(t_2, y_2)}{\partial(\varphi_1, y_1)} \end{bmatrix}.$$

For Type I orbits DP is given by the chain rule

$$\begin{bmatrix} \dfrac{\partial(t_2, y_2)}{\partial(\varphi_0, y_0)} \end{bmatrix} = \begin{bmatrix} \dfrac{\partial(t_2, y_2)}{\partial(\varphi_1, y_1)} \end{bmatrix} \begin{bmatrix} \dfrac{\partial(\varphi_1, y_1)}{\partial(\varphi_0, y_0)} \end{bmatrix}$$

$$= \begin{bmatrix} \dfrac{\partial(t_2, y_2)}{\partial(\varphi_1, y_1)} \end{bmatrix} \begin{bmatrix} 1 & 0 \\ 0 & -r \end{bmatrix} \tag{12}$$

where the first term comes from the free flight from $x = +1$ back to $x = +1$ and the second term from the impact rule. The details of the computations are given in the Appendix. For Type I motions we find that the determinant and trace of DP evaluated at the fixed point

(y_n, φ_n) are, respectively,

$$\det = [r \exp(-\alpha n T)]^2 \tag{13a}$$

$$tr = \frac{\exp(-\alpha n T)}{\Omega y_n}\left[-2ry_n\Omega\cosh(\Omega n T)\right.$$
$$\left.+(1+r)\sinh(\Omega n T)\left(-H_n\omega^2+y_n(G_n(1+\omega^2)+2\alpha I_n)\right)/H_n\right]. \tag{13b}$$

It follows from $\det \leqslant 1$ (since $r \leqslant 1$, $\alpha \geqslant 0$) that Type I motions cannot undergo Hopf bifurcations. The $\lambda = \pm 1$ bifurcations are given by the conditions

$$1 + \det \mp tr = 0 \qquad \text{for } \lambda = \pm 1. \tag{14}$$

Substitution of equations (13a, b) into (14) gives, after some algebra, a linear equation in y_n. The solutions of that equation are

$$y_n(\lambda = \pm 1) = \frac{\pm s_\Omega(1+r)\omega^2 H_n}{\Omega H_n[c_\alpha + s_\alpha + r^2(c_\alpha - s_\alpha)] \pm [s_\Omega(1+r)\{G_n(1+\omega^2)+2\alpha I_n\} - 2r\Omega H_n c_\Omega]} \tag{15}$$

where $s_\Omega = \sinh(\Omega n T)$, $c_\Omega = \cosh(\Omega n T)$, $s_\alpha = \sinh(\alpha n T)$ and $c_\alpha = \cosh(\alpha n T)$.

A substantial calculation verifies that the $y_n(\lambda = +1)$ value is simply the value of y_n at the saddle-node condition, $\beta_n^I(\mathrm{SN})$, equation (6). The $y_n(\lambda = -1)$ value corresponds to a value of y_n at which a period doubling occurs. In order to determine the driving amplitude β at which this secondary bifurcation occurs we rearrange equation (4a) to solve for β as a function of y_n. Then, by substituting in the value of $y_n(\lambda = -1)$ for y_n we obtain the following:

Theorem 6. Period doubling bifurcations of stable Type I motions of period nT occur at

$$\beta_n^I(\mathrm{PD}) = q\left[1 + \frac{(I_n^2 + \omega^2 G_n^2)y_n^2(\mathrm{PD}) - 2G_n H_n \omega^2 y_n(\mathrm{PD})}{\omega^2 H_n^2}\right]^{1/2} \tag{16}$$

where $y_n(\mathrm{PD}) = y_n(\lambda = -1)$.

As β is increased through $\beta_n^I(\mathrm{PD})$ both stable Type I motions of period nT become unstable and new motions having period $2nT$ and two impacts per period appear. It will be shown that $\beta_n^I(\mathrm{PD}) > \beta_n^I(\mathrm{SN})$ as expected (see Section 5.3 below).

5.2. *Type II motions*

Consider $(y_n, \varphi_n) \in \Sigma$ and the following conditions for the two pieces of the trajectory for a Type II motion

$$\begin{aligned}
(y_1, \varphi_1) &= (-ry_0, \varphi_0) \qquad \text{(impact)}\\
x(t_2; y_1, \varphi_1) &= -1\\
\dot{x}(t_2; y_1, \varphi_1) &= y_2\\
(y_3, t_3) &= (-ry_2, t_2) \qquad \text{(impact)}\\
x(t_4; y_3, t_3) &= 1\\
\dot{x}(t_4; y_3, t_3) &= y_4.
\end{aligned} \tag{17}$$

Then $\mathbf{P}(y_0, \varphi_0) = (y_4, t_4 (\mathrm{mod}\ T))$ and DP is given by

$$DP = DP_{43}\, DP_{32}\, DP_{21}\, DP_{10}$$

where

$$DP_{10} = DP_{32} \cdot \begin{bmatrix} 1 & 0 \\ 0 & -r \end{bmatrix}$$

and

$$DP_{ij} = \left[\frac{\partial(t_i, y_i)}{\partial(t_j, y_j)}\right] \qquad \text{with } (i,j) = (4,3) \text{ and } (2,1).$$

Again the details of the computation are in the Appendix and only the main results are provided here. The determinant and trace evaluated on a Type II fixed point are, respectively,

$$\det = [r \exp(-\alpha n T/2)]^4 \tag{18a}$$

$$\begin{aligned} \mathrm{tr} = \left(\frac{\exp(-\alpha n T/2)}{\Omega y_n}\right)\Big(& y_n^2[\sinh(\Omega n T/2)\,(2r^2\Omega^2 + \Delta^2(1+r)^2) \\ & + 4\cosh(\Omega n T/2)\sinh(\Omega n T/2)\,\Omega r\Delta(1+r) + \cosh^2(\Omega n T/2)\,2r^2\Omega^2] \\ & + y_n[2\Delta(1+r)^2\omega^2\sinh(\Omega n T/2) + 4\cosh(\Omega n T/2)\sinh(\Omega n T/2)\,\Omega r(1+r)\omega^2] \\ & + (1+r)^2\omega^4\sinh^2(\Omega n T/2)\Big) \end{aligned} \tag{18b}$$

where

$$\Delta = -\left[\frac{2\alpha K_n + L_n(1+\omega^2)}{J_n}\right].$$

Type II motions cannot undergo Hopf bifurcations since $\det < 1$. The $\lambda = \pm 1$ bifurcations conditions are found by using equation (14) which in this case yields a quadratic equation in y_n. The $\lambda = -1$ bifurcation conditions are non-physical, which follows from the symmetry of the Type II orbits. One of the two roots of the quadratic for $\lambda = +1$ corresponds to the saddle-node bifurcation value of y_n and the other corresponds to a secondary bifurcation which is in this case a pitchfork, or symmetric saddle-node, bifurcation. We denote the pitchfork bifurcation value of y_n as $y_n(\mathrm{PF})$. Solving for the corresponding β value as was done for Type I motions yields:

Theorem 7. Pitchfork bifurcations of Type II motions occur at β values of

$$\beta_n^{II}(\mathrm{PF}) = q\left[1 + \frac{(K_n^2 + \omega^2 L_n^2)\,y_n^2(\mathrm{PF}) - 2L_n J_n \omega^2 y_n(\mathrm{PF})}{\omega^2 J_n^2}\right]^{1/2} \tag{19}$$

As β is increased through $\beta_n^{II}(\mathrm{PF})$, the stable Type II motion of period nT becomes unstable and an antisymmetric pair of stable motions of period nT appear. As expected, $\beta_n^{II}(\mathrm{PF}) > \beta_n^{II}(\mathrm{SN})$ as is shown below.

5.3. *Summary*

Figure 5 shows bifurcation curves for Type I and II motions. Note that as n becomes large the secondary bifurcations occur very close to the saddle-node bifurcations and that the curves of all bifurcation types accumulate onto β_∞ as $n \to \infty$. In Chow and Shaw [7] explicit asymptotic calculations were done for the separation of the primary and secondary bifurcation curves for large n. This was possible since the calculations for the secondary bifurcation conditions were more tractable for that (similar) system. The conclusions drawn in [7] are valid for the present system as well: the "window of stability" for which a period nT motion exists *and* is stable shrinks exponentially as n increases. Hence the secondary bifurcation curves also converge to β_∞ as $n \to \infty$. This is quite easily proved by computing the following limits:

$$\begin{aligned} \lim_{n\to\infty} y_n(\mathrm{PF}) &= \lim_{n\to\infty} y_n(\mathrm{PD}) = \lim_{n\to\infty} y_n^I(\mathrm{SN}) = \lim_{n\to\infty} y_n^{II}(\mathrm{SN}) \\ &= \frac{2\omega^2\Omega(1+r)}{\omega^2(1+r)^2 + [\alpha(1+r) + \Omega(1-r)]^2} \end{aligned} \tag{20}$$

where $y_n^j(\mathrm{SN})$ is the y_n value at the saddle-node bifurcation point for a Type j motion ($j = \mathrm{I}, \mathrm{II}$).

In all cases secondary bifurcations occur at values of β larger that the associated saddle-node values. This is shown as follows. Let y_s denote the value of y_n at a secondary bifurcation, i.e. $y_n(\mathrm{PD})$ or $y_n(\mathrm{PF})$. Then y_s must satisfy the quadratic equation (4a) or (9a) at

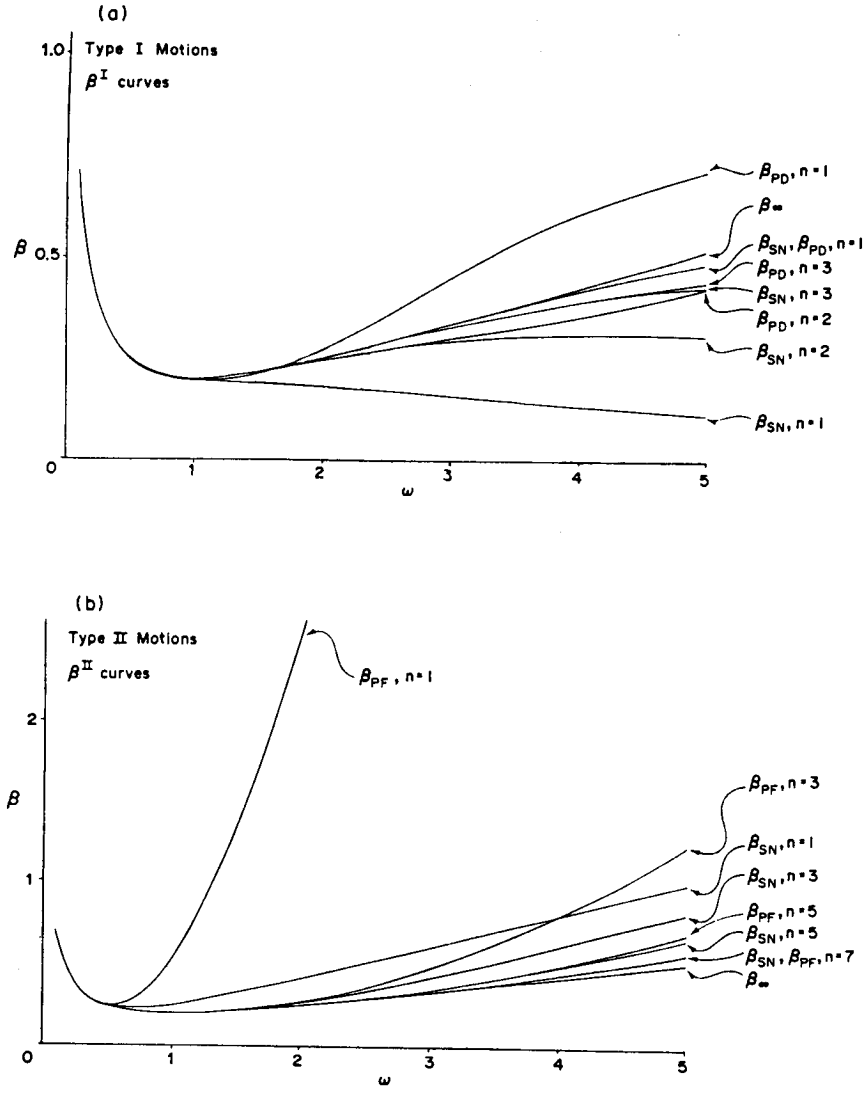

Fig. 5. Bifurcation diagrams in (β, ω) space, $r = 1.0$, $\alpha = 0.2$. (a) Type I motions. (b) Type II motions. SN = saddle node, PD = period doubling, PF = pitchfork.

$\beta = \beta_s = \beta_n^I(\mathrm{PD})$ or $\beta_n^{II}(\mathrm{PF})$, respectively. Writing the quadratic as $Ay_s^2 + By_s + C[1 - (\beta_s/q)^2] = 0$, β_s can be expressed as

$$\beta_s = q\left[\frac{4AC - B^2 + (2Ay_s + B)^2}{4AC}\right]^{1/2}.$$

The saddle-node value of β is simply $\beta(\mathrm{SN}) = q\left[\frac{4AC - B^2}{4AC}\right]^{1/2}$ and since $4AC > B^2 > 0$ in both cases, it follows that $\beta_s > \beta(\mathrm{SN})$.

The limit $\omega \to \infty$ for finite n shows that the Type I saddle-node bifurcation curves, $\beta_n^I(\mathrm{SN})$, diverge from the β_∞ curve. This can be seen by considering

$$\beta_\infty \approx \omega\left[\frac{1-r}{1+r}\Omega + \alpha\right] \quad \text{as } \omega \to \infty$$

and

$$\lim_{\omega \to \infty} \beta_n^I(\mathrm{SN}) = \left[\frac{\pi n(1-r)}{(1+r)}\right].$$

Thus if n is fixed and $\omega \to \infty$, the β_n^I(SN) curve will flatten out while the β_∞ curve continues to grow. Plots of β_n^I(PD) indicate that these also are asymptotic to a constant value (which depends on n) although the details have not been worked out. In addition, β_n^{II} (SN) curves grow like ω^2 for large ω and thus also diverge from β_∞ for fixed n.

6. MELNIKOV ANALYSIS

In this section we present an exact calculation of the separation of the stable and unstable manifolds of the periodic orbit $(\tilde{x}, \tilde{y})$ discussed in Section 3. A similar calculation can be found in [7].

Referring to Fig. 6, for $\beta < q$ the period T motion $(\tilde{x}, \tilde{y})$ is not affected by impacts at $|x| = 1$, and one branch of its unstable manifold W^u, intersects Σ in a curve denoted by $y^u(\varphi)$. Its stable manifold, W^s, first "reaches back" to $x = +1$ at $y^s(\varphi) < 0$ as shown. Taking W^s one step further back, under the inverse of the impact rule, its intersection with Σ is given by $-1/ry^s(\varphi)$. Thus the separation between W^u and W^s in Σ is given by the distance function (see [12], Chap. 4)

$$\Delta(\varphi) = y^u(\varphi) + \frac{1}{r} y^s(\varphi). \tag{21}$$

If $\Delta(\varphi)$ has no zeros then W^s and W^u do not intersect, while if $\Delta(\varphi)$ has simple zeros then W^s and W^u intersect transversally. Such transversal intersections imply the existence of horseshoes via the Smale–Birkhoff homoclinic theorem [12, p. 252]. In the non-generic intermediate case in which $\Delta(\varphi)$ has quadratic zeros (double roots), W^s and W^u intersect with quadratic tangencies.

To compute $y^u(\varphi)$, consider trajectories starting in Σ which approach $(\tilde{x}, \tilde{y})$ as $t \to -\infty$. It is convenient to write the solution of (1a) as

$$x(t; 1, y_0, \varphi) = c_1 e^{s_1(t-\varphi)} + c_2 e^{s_2(t-\varphi)} + \beta/q \cos(\omega t + \psi)$$

where

$$s_1(>0) = -\alpha + \Omega, \qquad s_2(<0) = -\alpha - \Omega,$$

$$c_1 = \left[y_0 + \frac{\beta}{q}\omega \sin(\omega\varphi + \psi) + s_2\left(\frac{\beta}{q}\cos(\omega\varphi + \psi) - 1\right)\right]/2\Omega$$

$$c_2 = -\left[y_0 + \frac{\beta}{q}\omega \sin(\omega\varphi + \psi) + s_1\left(\frac{\beta}{q}\cos(\omega\varphi + \psi) - 1\right)\right]/2\Omega.$$

In order for (y_0, φ) to be in W^u it must hold that $c_2 = 0$ since $s_2 < 0$. Requiring $x(\varphi; 1, y_0, \varphi) = 1$ and $c_2 = 0$ implies $c_1 = 1 - \beta/q \cos(\omega\varphi + \psi)$ and comparison of this with

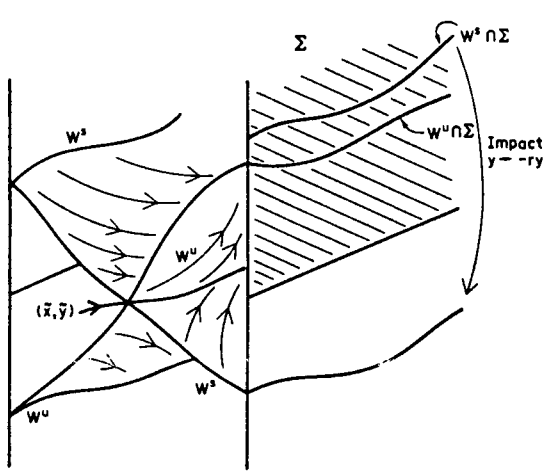

Fig. 6. Branches of the stable and unstable manifolds of $(\tilde{x}, \tilde{y})$ in the extended phase space (x, y, φ).

the expression for c_1 above yields

$$y^u(\varphi) = s_1\left[1 - \frac{\beta}{q}\cos(\omega\varphi + \psi)\right] - \frac{\beta}{q}\omega\sin(\omega\varphi + \psi). \tag{22}$$

$y^s(\varphi)$ is treated similarly: trajectories are considered which start at $x = +1$, $y_0 < 0$ and approach $(\tilde{x}, \tilde{y})$ as $t \to \infty$. In this case $c_1 = 0$ since $s_1 > 0$. Requiring $x(\varphi; 1, y_0, \varphi) = 1$ and $c_1 = 0$ implies $c_2 = 1 - \beta/q\cos(\omega\varphi + \psi)$ and comparing this with the general expression for c_2 above gives

$$y^s(\varphi) = s_2\left[1 - \frac{\beta}{q}\cos(\omega\varphi + \psi)\right] - \frac{\beta}{q}\omega\sin(\omega\varphi + \psi). \tag{23}$$

Now computing $\Delta(\varphi)$, using equation (21), results in

$$\Delta(\varphi) = -\frac{1}{r}\left[\left(1 - \frac{\beta}{q}\cos(\omega\varphi + \psi)\right)[\alpha(1+r) + \Omega(1-r)] + \frac{\beta}{q}\omega(1+r)\sin(\omega\varphi + \psi)\right] \tag{24}$$

or

$$\Delta(\varphi) = -\frac{1}{r}\left[\alpha(1+r) + \Omega(1-r)\right] + \frac{\beta}{q}\left[[\alpha(1+r) + \Omega(1-r)]^2 + [\omega(1+r)]^2\right]^{1/2}$$
$$\sin(\omega\varphi + \psi + \theta)$$

where θ is an easily computable phase angle. Considering the mean and oscillating parts of $\Delta(\varphi)$ gives the following result:

Theorem 8. The stable and unstable manifolds of $(\tilde{x}, \tilde{y})$, W^s and W^u, intersect with a quadratic tangency if and only if $\Delta(\varphi)$ has quadratic zeros or, equivalently,

$$\beta = \beta_\infty = \frac{q|(1-r)\Omega + (1+r)\alpha|}{[(1-r)\Omega + (1+r)\alpha]^2 + [\omega(1+r)]^2]^{1/2}}. \tag{25}$$

Also, W^s and W^u intersect transversally if and only if $\Delta(\varphi)$ has simple zeros or, equivalently, $\beta > \beta_\infty$.

Remarks

(1) This recaptures, by another method, the appearance of non-periodic motions in the system.

(2) The saddle orbit $(\tilde{x}, \tilde{y})$ is non-impacting for $\beta < q$ only. From (25) it is easily seen that $\beta_\infty < q$ and it is expected that for $\beta > q > \beta_\infty$ the stable manifolds of the impacting continuation of $(\tilde{x}, \tilde{y})$ will also intersect.

(3) For $\beta > \beta_\infty$ complicated dynamics may be expected for this system. Specifically, the existence of Smale horseshoes (cf. [12], Chap. 5) implies that an infinite number of non-periodic and periodic motions exist for $\beta > \beta_\infty$. These motions are unstable but can be the source of irregular, and frequently persistent, motions.

(4) Stable Type I and II motions can exist for $\beta > \beta_\infty$. Thus $\beta \geqslant \beta_\infty$ is not a sufficient condition for sustained chaotic motions, or strange attractors, to occur.

7. SIMULATIONS

The simulations are similar to those used in other works by the first author [8, 9]. The known solutions of the linear equations, the impact rule, and a simple root solving technique are combined to form a numerically stable simulation routine. The simulation is used here to demonstrate some of the analytical results of the previous sections.

Figure 4a, b shows results of the saddle-node bifurcations for motions of Types I and II (only stable motions are presented here). Figure 7a indicates the result of a period doubling bifurcation of a Type I motion. Figure 7b depicts a motion after a pitchfork bifurcation of the Type II motion. Figure 7c shows a strange attractor type motion, for $\beta > \beta_\infty$, in the phase plane. Figure 7d shows the same motion for a longer duration as an orbit of the map **P**, i.e. as points in Σ. Figure 8 shows branches of the curves $y^s(\varphi) = W^s \cap \Sigma$ and $y^u(\varphi) = W^u \cap \Sigma$ exhibiting the quadratic tangency of Theorem 8 at $\beta = \beta_\infty$, cf. Fig. 6.

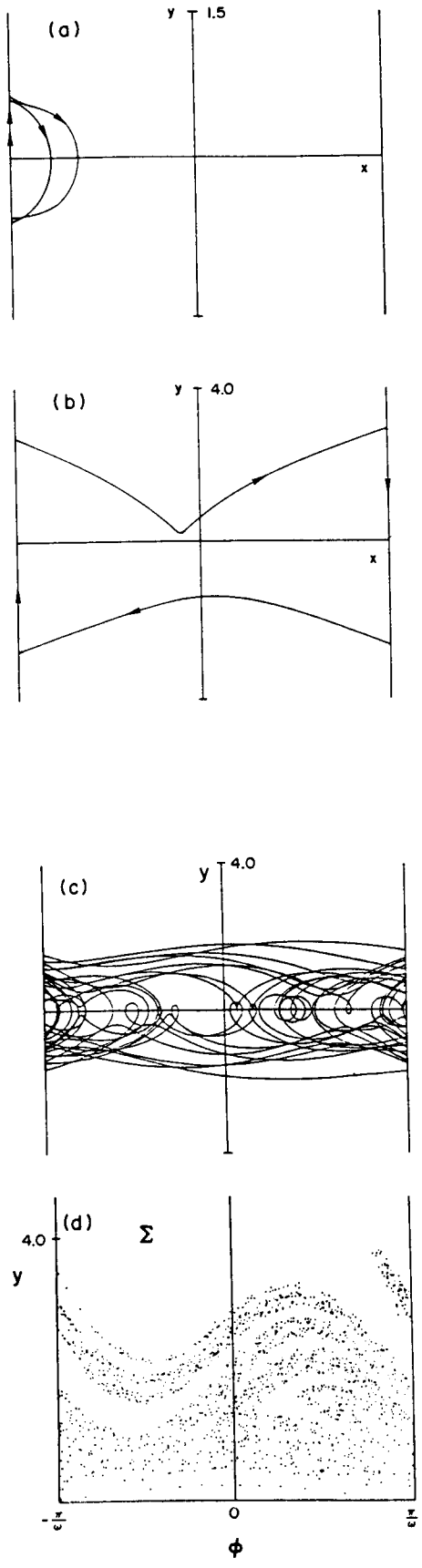

Fig. 7. Simulations, $r = 1.0$, $\alpha = 0.1$. (a) Period $2T$ motion, $\beta = 0.65$, $\omega = 4.0$. (b) Unsymmetric period T motion, $\beta = 2.3$, $\omega = 1.8$. (c) Apparently chaotic motion, $\beta = 2.0$, $\omega = 4.0$. (d) Motion from (c) as seen in Σ.

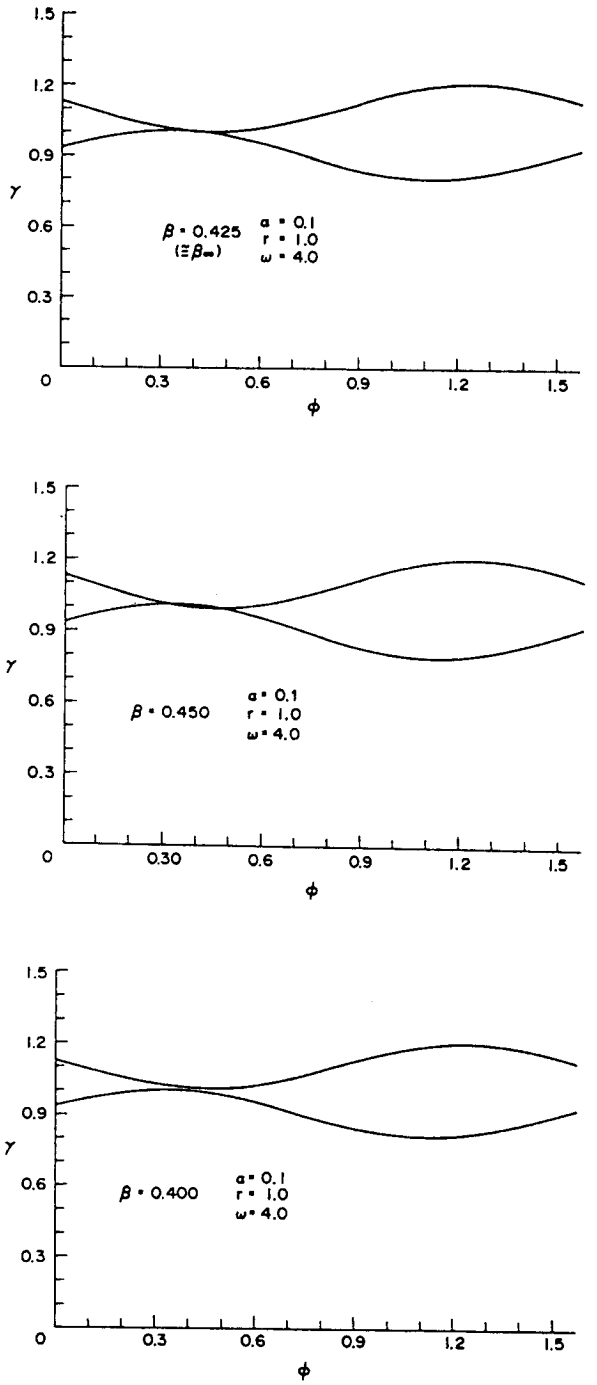

Fig. 8. Simulation, $r = 1.0$, $\alpha = 0.1$, $\omega = 4.0$ ($\beta = 0.425 \approx \beta_\infty$). Branches of the curves $y^s(\varphi) = W^s \cap \Sigma$ and $y^u(\varphi) = W^u \cap \Sigma$ are displayed in Σ, cf. Fig. 6.

8. DISCUSSION

The period doubling of each Type I motion and the pitchfork bifurcation of each Type II motion is followed by its own Feigenbaum period doubling sequence [14]. For $n \to \infty$ these sequences accumulate onto β_∞ for both types of motions.

Figure 5 indicates that stable motions of Types I and II of low subharmonic order n exist above the infinite sequence of bifurcations occurring near β_∞. This implies that β_∞ is not a condition for the appearance of steady-state chaos (i.e. strange attractors), but simply for *transient* chaos, (i.e. horseshoes). There are no immediately obvious parameter conditions for which one can expect strange attractors to occur. For large values of β the motions

considered in this study will be unstable (i.e. after each Feigenbaum sequence is completed) but other stable motions will undoubtedly appear via saddle-node bifurcations.

The accumulation of saddle-node and secondary bifurcations near points of homoclinic tangency can be shown to occur in general by using qualitative arguments based on the quadratic nature of the tangency, see the discussion in Guckenheimer and Holmes [12], Section 6.6. Chow and Shaw [7] compare explicit results, similar to those obtained here, with the estimates given in [12].

Many researchers beginning to study non-linear systems overlook some crucial points demonstrated by this example. Firstly, there are to date no methods to provide necessary and sufficient conditions for a strange attractor to exist. Although the existence of horseshoes gives the possibility of chaos, one cannot conclude the existence of a strange attractor without additional information regarding the *attractivity* of the strange set. Secondly, the existence of a strange attractor (or of any stable steady-state for that matter) does not preclude the existence of other steady states. These competing attractors often have domains of attraction with fractal boundaries. In fact, Melnikov's method is useful in predicting the creation of fractal basin boundaries which separate motions which end up interacting only with the $+1$ (or -1) barriers, i.e. it provides for the onset of sensitive dependence of initial conditions which can exist in the absence of a strange attractor. This is often referred to as transient chaos or preturbulence.

Finally, we note that the physical system analysed in this paper is quite simple to construct. Experiments on such a system have demonstrated many of the phenomena described above and specific bifurcation conditions have been verified [13].

Acknowledgement—The authors wish to thank Pi-Cheng Tung for assistance with the graphs and simulations presented in this work.

REFERENCES

1. S. N. Chow, J. K. Hale and J. Mallet-Paret, An example of bifurcation to homoclinic orbits. *J. diff. Eqns* **37**, 351–373 (1980).
2. B. Greenspan and P. Holmes, Homoclinic orbits, subharmonics and global bifurcations in forced oscillations. *Nonlinear Dynamics and Turbulence* (Edited by G. Barablatt, G. Iooss and D. Joseph). Pitman Press, London (1983).
3. F. C. Moon, *Chaotic Vibrations*. Wiley, NY (1987).
4. F. Moon and P. Holmes, A magnetoelastic strange attractor. *J. Sound Vibrat.* **65**, 275–296 (1979).
5. P. Holmes, A non-linear oscillator with a strange attractor. *Phil. Trans. R. Soc.* **A292**, 419–448 (1979).
6. F. M. A. Salam, The Melnikov technique for highly dissipative systems. *SIAM J. appl. Math.*, **47**, 232–243 (1987).
7. S. N. Chow and S. W. Shaw, Bifurcations of subharmonics. *J. diff. Eqns*, **65**, 304–320 (1986).
8. S. W. Shaw and P. J. Holmes, A periodically forced piecewise linear oscillator. *J. Sound Vibrat.* **90**, 129–155 (1983).
9. S. W. Shaw, The dynamics of a harmonically excited systems having rigid amplitude constraints, Part I: subharmonic motions and local bifurcations. *J. appl. Mech.* **52**, 453–458.
10. S. W. Shaw and P. J. Holmes, Periodically forced linear oscillator with impacts—chaos and long period motions. *Phys. Rev. Lett.* **51**, 623–626.
11. G. S. Whitson, Global dynamics of a vibro-impacting linear oscillator. *J. Sound Vibrat.* **118**, 395–429 (1987).
12. J. Guckenheimer and P. Holmes, *Nonlinear Oscillations, Dynamical Systems and Bifurcations of Vector Fields*. Springer, NY (1983).
13. D. Moore and S. W. Shaw, Experimental response of a single degree of freedom impacting system. *Proceedings of the 20th of the Midwest Mechanics Conference*, pp. 839–844 (1987).
14. M. Feigenbaum, Quantitative universality for a class of nonlinear transformations. *J. stat. Phys.* **19**, 25–52.

APPENDIX: SOME DETAILS OF THE STABILITY CALCULATIONS

For similar calculations see [6–8].

Type I motions

The implicit form of the map **P** for Type I motions is given by equation (11) along with $(\varphi_1, y_1) = (\varphi_0, \cdot\cdot ry_0)$. Then the first derivative of **P** is determined from the chain rule to be

$$DP = DP_{21}\,DP_{10} = \begin{bmatrix} \partial(t_2, y_2) \\ \partial(\varphi_1, y_1) \end{bmatrix} \begin{bmatrix} 1 & 0 \\ 0 & -r \end{bmatrix} \tag{A1}$$

using the notation of Section 5.1. The term DP_{21} is determined using implicit differentiation on conditions (11) and

gives

$$\frac{\partial t_2}{\partial t_1} = e_{21}[\Omega y_1 c_{21} + (\alpha y_1 + a_1)s_{21}]/\Omega y_2$$

$$\frac{\partial t_2}{\partial y_1} = -e_{21}s_{21}/\Omega y_2$$

$$\frac{\partial y_2}{\partial t_1} = e_{21}[(y_1 a_2 - y_2 a_1)\Omega c_{21} + [a_2 a_1 - y_2 y_1 + \alpha(y_1 a_2 + a_1 y_2)]]/\Omega y_2$$

$$\frac{\partial y_2}{\partial y_1} = e_{21}[\Omega y_2 c_{21} - (\alpha y_2 + a_2)s_{21}]/\Omega y_2 \tag{A2}$$

where

$$e_{ij} = \exp[-\alpha(t_i - t_j)],$$
$$c_{ij} = \cosh[\Omega(t_i - t_j)],$$
$$s_{ij} = \sinh[\Omega(t_i - t_j)],$$
$$a_i = \beta\cos(\omega t_i) + 1 - 2\alpha y_i$$
$$\varphi_1 = t_1 \pmod T.$$

To evaluate these on a periodic Type I motion we use $c_{21} = \cosh(\Omega n T)$, $s_{21} = \sinh(\Omega n T)$, $e_{21} = \exp(-\alpha n T)$, $y_1 = -ry_n$, $y_2 = y_n$, $a_1 = \beta\cos(\omega\varphi_n) + 1 + 2\alpha r y_n$ and $a_2 = \beta\cos(\omega\varphi_n) + 1 - 2\alpha y_n$.

Computation of the determinant and trace of DP follows in a straightforward manner from this point. However, to obtain these in terms of y_n and the system parameters alone, the terms involving $\cos(\omega\varphi_n)$ must be dealt with. In order to replace this with an expression involving only y_n we use the identity

$$\cos(\omega\varphi_n) = \cos[(\omega\varphi_n + \psi) - \psi] = \cos(\omega\varphi_n + \psi)\cos(\psi) + \sin(\omega\varphi_n + \psi)\sin(\psi).$$

The trigonometric terms involving $(\omega\varphi_n + \psi)$ are known in terms of y_n as given in equations (4b, c) and those involving (ψ) are easily found to be $\sin(\psi) = -2\alpha\omega/q$ and $\cos(\psi) = -(1 + \omega^2)/q$ from the particular solution of equation (1a). These results allow one to obtain the trace and determinant in terms of y_n and the parameters as given in (13a, b).

Type II motions

For Type II motions the implicit form of **P** is given by equation (17). For DP_{21} expressions (A2) are valid with $a_1 = \beta\cos(\omega t_1) + 1 - 2\alpha y_1$, and $a_2 = \beta\cos(\omega t_2) - 1 - 2\alpha y_2$. These expressions are also valid for DP with the subscripts changed from (2, 1) to (4, 3). Evaluation on a Type II periodic motion requires $c_{43} = c_{21} = \cosh(\Omega n T/2)$, $s_{43} = s_{21} = \sinh(\Omega n T/2)$, $e_{43} = e_{21} = \exp(-\alpha n T/2)$, $a_1 = -a_3 = \beta\cos(\omega\varphi_n) + 1 + 2\alpha r y_n$, $a_2 = -a_4 = -\beta\cos(\omega\varphi_n) + 2\alpha y_n - 1$, $y_1 = -ry_n$, $y_2 = -y_n$, $y_3 = ry_n$, and $y_4 = y_n$. Carrying out the matrix multiplication for DP indicated in Section 5.2 and computing the determinant and trace provides expressons (18 a, b). This is a substantial calculation and requires writing $\cos(\omega\varphi_n)$ in terms of y_n as was done for the analysis of Type I motions.